JOURNAL OF GUIDANCE, CONTROL, AND DYNAMICS
Vol. 33, No. 4, July–August 2010

Optimal Intercept Missile Guidance Strategies with Autopilot Lag

Robert H. Chen*
Northrop Grumman Corporation, El Segundo, California 90245
Jason L. Speyer†
SySense, Inc., El Segundo, California 90245
and
Dimitrios Lianos‡
U.S. Army Research, Development, and Engineering Command, Huntsville, Alabama 35806

DOI: 10.2514/1.44618

In the linear-quadratic pursuit-evasion game, the pursuer (interceptor) wishes to minimize the terminal miss, whereas the evader (target) wishes to maximize it. Therefore, the optimal strategy of the interceptor is derived against the anticipated worst possible strategy of the target. If the interceptor has a lag, the current approach is to include this lag directly in the system dynamics, which are known to both players. In this problem formulation, the optimal cost could easily go to infinity, which means that the target will win the game. This is expected, because the target has knowledge about interceptor's lag. To ensure the existence of an interceptor strategy, the weighting on the terminal miss has to be chosen small enough so that the optimal cost will remain finite. However, this manipulation prevents the target from maximizing the terminal miss and effectively constrains the target strategy. Therefore, the interceptor strategy is derived against the worst-case target strategy that is not really the worst case. In this paper, it is shown that this interceptor strategy performs poorly in realistic situations where the target tries to maximize the terminal miss. Instead, two new interceptor strategies are derived against target strategies that are determined without knowledge about the interceptor's lag. These two optimal interceptor strategies improve the game-theoretic guidance law for homing missiles by correctly taking into account the autopilot lag.

I. Introduction

HOMING missile guidance has been an important area of research in the past few decades. Because proportional navigation [1–4] incurs large miss distance in the presence of maneuvering targets, many advanced guidance laws have been developed by using two different methods. One method is to use the target model in which the target is assumed to perform a certain maneuver. For example, the augmented proportional navigation is derived, assuming that the target acceleration is constant in an inertial direction [3–6]. More realistic guidance laws are derived, assuming that the target acceleration vector may rotate but is orthogonal to the target velocity vector, and its magnitude is either constant [7] or sinusoidal [8]. The other method is to use the differential game in which the target is assumed to be intelligent and tries to maximize the miss distance. This is the well-known linear-quadratic pursuit-evasion game [2,4]. In the problem formulation, the pursuer (interceptor) wishes to minimize the terminal miss, whereas the evader (target) wishes to maximize it. Therefore, the optimal interceptor strategy is derived against the anticipated worst-possible-target strategy.

Because the acceleration command generated by the guidance law is realized by the control law (autopilot), which tracks the acceleration command by modulating the interceptor's fins or thrusters, there always exists a lag between desired and achieved accelerations. Therefore, the interceptor's performance can be improved by using a guidance law that takes into account this autopilot lag, which is usually modeled as first-order dynamics. For guidance laws that use the target model, it is rather straightforward to include the interceptor's lag [3–5,8]. For the game-theoretic guidance law, the current approach is to include the interceptor's lag directly in the system dynamics [4,9,10]. In this problem formulation, because the system dynamics are known to both players, the target strategy is determined with the knowledge about the interceptor's lag. Then, the target may maneuver at a small time-to-go to produce large terminal miss, knowing that the interceptor will not have enough time to respond due to its lag. Therefore, if a large weighting is placed on the terminal miss, the optimal cost could go to infinity, which means that the target will win the game, even though the target is less maneuverable than the interceptor. This is consistent with the finite escape time of the associated Riccati equation. To ensure the existence of an interceptor strategy, the weighting on the terminal miss has to be chosen to be small enough so that the optimal cost will remain finite. However, this manipulation prevents the target from maximizing the terminal miss and effectively constrains the target strategy. Therefore, the interceptor strategy is derived against the worst-case target strategy that is not really the worst case. This interceptor strategy will not perform well against targets that intend to maximize the terminal miss. In a realistic engagement scenario, shown later, where the target performs a simple maneuver, this interceptor strategy performs much worse than the classic interceptor strategy, which does not consider the interceptor's lag. This interceptor strategy also performs much worse than the proportional navigation that considers the interceptor's lag.

In this paper, a new approach is proposed to improve the game-theoretic guidance law in the presence of autopilot lag. Instead of being determined together in one optimization problem, the interceptor strategy and target strategy are determined separately in two optimization problems. First, the target strategy is derived in a two-sided optimization problem that does not consider the interceptor's lag. Then, the interceptor strategy is derived in a one-sided optimization problem that considers the interceptor's lag subject to the target strategy derived in the first optimization problem. In this problem formulation, the target strategy is determined, assuming that the interceptor does not have a lag. Therefore, the

Presented as Paper 6535 at the AIAA Guidance, Navigation, and Control Conference, Hilton Head, SC, 20–23 August 2007; received 28 March 2009; revision received 14 February 2010; accepted for publication 13 April 2010. Copyright © 2010 by Robert H. Chen. Published by the American Institute of Aeronautics and Astronautics, Inc., with permission. Copies of this paper may be made for personal or internal use, on condition that the copier pay the $10.00 per-copy fee to the Copyright Clearance Center, Inc., 222 Rosewood Drive, Danvers, MA 01923; include the code 0731-5090/10 and $10.00 in correspondence with the CCC.

*Senior Research Engineer, Aerospace Systems Sector. Senior Member AIAA.
†Chief Technology Officer; Professor, University of California, Los Angeles, California 90095. Fellow AIAA.
‡Missile Specialist, Missile Research, Development, and Engineering Center. Member AIAA.

interceptor strategy derived in the presence of interceptor's lag against this target strategy is more realistic and effective. However, this new problem formulation does not have a saddle point condition because of the additional dynamics of the interceptor's lag. Therefore, this new interceptor strategy is considered as the worst-case design, where the target is perverse enough to determine its worst strategy but is not perverse enough to actually change its strategy as the game evolves [2]. In other words, it is implicitly assumed that the target plays first by announcing its strategy ahead of time. Note that, if the second optimization problem does not consider the interceptor's lag, this new interceptor strategy is equivalent to the classic interceptor strategy. Finally, another interceptor strategy is derived where the second optimization problem considers the target strategy as an open-loop strategy instead of a closed-loop strategy. That is, the target strategy is a function of the states of the first optimization problem instead of in feedback form as a function of the states of the second optimization problem. Therefore, the target assumes that the interceptor plays optimally, as in the first optimization problem, and will not take advantage of any nonoptimal play made by the interceptor [2]. While the interceptor strategy derived against the open-loop target strategy satisfies a less stringent type of optimality, it can be solved in closed form, which significantly reduces the computation.

This paper is organized as follows. In Sec. II, the differential game and linear-quadratic pursuit-evasion game are reviewed. In Sec. III, the linear-quadratic pursuit-evasion game is formulated when the interceptor has a lag. In Secs. IV and V , the optimal interceptor strategies are derived against closed-loop and open-loop target strategies, respectively. In Sec. VI, the two proposed guidance laws are demonstrated in a numerical example where the three-dimensional guidance law is equivalent to two two-dimensional guidance laws through a decomposition of the three-dimensional relative motion between the target and the interceptor into two two-dimensional planes.

II. Background

A. Differential Game

Consider the linear differential game [2],

$$\min_{u_1}\max_{u_2} J$$

where the cost is

$$J=\frac{1}{2}x(t_f)^T Q_f x(t_f)+\frac{1}{2}\int_{t_0}^{t_f}(x^T Qx+u_1^T R_1 u_1-u_2^T R_2 u_2)\,\mathrm{d}t \quad (1)$$

subject to the dynamics

$$\dot{x}=Ax+B_1u_1+B_2u_2 \quad (2)$$

where x is the state, u_1 is the pursuer's control, and u_2 is the evader's control. Q, R_1, R_2, and Q_f are designing weightings. By using the calculus of variations, the first-order necessary condition produces the optimal solutions:

$$u_1^*=-R_1^{-1}B_1^T\bar{\lambda} \quad (3a)$$

$$u_2^*=R_2^{-1}B_2^T\bar{\lambda} \quad (3b)$$

and the dynamic equation for the Lagrange multiplier

$$\dot{\bar{\lambda}}=-A^T\bar{\lambda}-Qx \quad (4)$$

where $\bar{\lambda}(t_f)=Q_f x(t_f)$. By using the sweep method, where $\bar{\lambda}\triangleq Sx$, the optimal solutions can be written as

$$u_1^*=-R_1^{-1}B_1^T Sx \quad (5a)$$

$$u_2^*=R_2^{-1}B_2^T Sx \quad (5b)$$

where S satisfies the Riccati equation:

$$-\dot{S}=SA+A^TS+Q-S(B_1R_1^{-1}B_1^T-B_2R_2^{-1}B_2^T)S \quad (6)$$

and $S(t_f)=Q_f$. Finally, by solving the two auxiliary problems [2], it can be shown that the pursuer and evader strategies in Eq. (5) satisfy the saddle point condition; that is,

$$J(u_1^*,u_2)\le J(u_1^*,u_2^*)\le J(u_1,u_2^*)$$

B. Linear-Quadratic Pursuit-Evasion Game

Consider the one-dimensional relative dynamics between the target and interceptor in the direction that is orthogonal to the nominal line of sight (LOS), as shown in Fig. 1 [2,4]:

$$\dot{\bar{x}}=v \quad (7a)$$

$$\dot{v}=a_T-a_I \quad (7b)$$

where $\bar{x}$ is the relative position, v is the relative velocity, a_T is the target acceleration, and a_I is the interceptor acceleration. The linear-quadratic pursuit-evasion game is [2,4]

$$\min_{a_I}\max_{a_T}\left\{\frac{1}{2c}\bar{x}(t_f)^2+\frac{1}{2}\int_{t_0}^{t_f}[a_I(t)^2-\gamma a_T(t)^2]\,\mathrm{d}t\right\} \quad (8)$$

subject to Eq. (7), where $c^{-1}>0$ is the design weighting on the terminal miss and $\gamma>1$ is the design weighting on the maneuverability of the target. Note that it is assumed that the interceptor is more maneuverable than the target. When $\gamma\to\infty$, the target is nonmaneuvering.

By comparing Eqs. (7) and (8) with Eqs. (1) and (2), the state, the pursuer's control, and the evader's control are

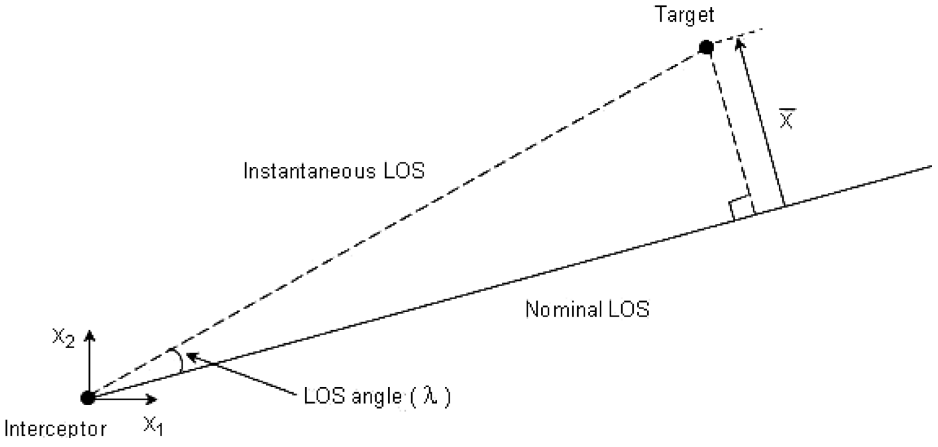

Fig. 1 One-dimensional relative motion between target and interceptor in two-dimensional plane.

$$x = \begin{bmatrix} \bar{x} \\ v \end{bmatrix}; \qquad u_1 = a_I; \qquad u_2 = a_T$$

with system matrices

$$A = \begin{bmatrix} 0 & 1 \\ 0 & 0 \end{bmatrix}; \qquad B_1 = \begin{bmatrix} 0 \\ -1 \end{bmatrix}; \qquad B_2 = \begin{bmatrix} 0 \\ 1 \end{bmatrix}$$

and design weightings

$$Q = 0; \qquad R_1 = 1; \qquad R_2 = \gamma; \qquad Q_f = \begin{bmatrix} c^{-1} & 0 \\ 0 & 0 \end{bmatrix}$$

By substituting the system matrices and design weightings into Eq. (6), the Riccati matrix can be solved in closed form as

$$S(t) = \frac{3}{(1-\gamma^{-1})T_{\text{go}}^3 + 3c} \begin{bmatrix} 1 & T_{\text{go}} \\ T_{\text{go}} & T_{\text{go}}^2 \end{bmatrix} \tag{9}$$

where $T_{\text{go}} \triangleq t_f - t$ is the time-to-go. Then, by using Eq. (5a), the guidance law for the interceptor is

$$a_I^*(t) = \frac{3T_{\text{go}}}{(1-\gamma^{-1})T_{\text{go}}^3 + 3c}[\bar{x}(t) + T_{\text{go}} v(t)] \tag{10}$$

Note that this interceptor acceleration is applied in the direction that is orthogonal to the nominal LOS.

For this set of system matrices and design weightings, Eqs. (3) and (4) can also be solved directly as follows. By integrating Eq. (4),

$$\bar{\lambda}(t) = \frac{1}{c} \begin{bmatrix} 1 \\ T_{\text{go}} \end{bmatrix} \bar{x}(t_f) \tag{11}$$

By substituting Eq. (11) into Eq. (3), the interceptor strategy and target strategy are

$$a_I^*(t) = \frac{T_{\text{go}}}{c} \bar{x}(t_f) \tag{12a}$$

$$a_T^*(t) = \frac{T_{\text{go}}}{\gamma c} \bar{x}(t_f) \tag{12b}$$

To implement Eq. (12a), the interceptor acceleration needs to be expressed in terms of the current state instead of the final state. By integrating Eq. (7) with Eq. (12),

$$\bar{x}(t_f) = \left[1 + \frac{(1-\gamma^{-1})T_{\text{go}}^3}{3c}\right]^{-1} [\bar{x}(t) + T_{\text{go}} v(t)] \tag{13}$$

Then, by substituting Eq. (13) into Eq. (12a), the guidance law for the interceptor is obtained, which is equivalent to Eq. (10), as expected.

Remark 1: From Fig. 1, the LOS rate is

$$\dot{\lambda} = \frac{\mathrm{d}}{\mathrm{d}t}\left(\tan^{-1}\frac{\bar{x}}{V_c T_{\text{go}}}\right) = \frac{\bar{x} + T_{\text{go}} v}{V_c T_{\text{go}}^2} \tag{14}$$

where V_c is the closing velocity (i.e., the relative velocity along the nominal LOS) assumed to be constant [2,4]. By using Eq. (14), Eq. (10) can be written as

$$a_I^* = N V_c \dot{\lambda} \tag{15}$$

where

$$N = \frac{3T_{\text{go}}^3}{(1-\gamma^{-1})T_{\text{go}}^3 + 3c} \tag{16}$$

is the navigation ratio. Note that

$$\lim_{c \to 0} N = \lim_{T_{\text{go}} \to \infty} N = \frac{3}{1-\gamma^{-1}}$$

When $\gamma \to \infty$ and $c \to 0$, Eqs. (10) and (15) become

$$a_I^* = \frac{3}{T_{\text{go}}^2}(\bar{x} + T_{\text{go}} v) = 3V_c \dot{\lambda}$$

which is equivalent to the proportional navigation [2–4].

Remark 2: If the two-dimensional relative dynamics, as shown in Fig. 1, are considered instead of the one-dimensional relative dynamics,

$$\dot{x}_1 = v_1; \qquad \dot{x}_2 = v_2; \qquad \dot{v}_1 = a_{T_1} - a_{I_1}; \qquad \dot{v}_2 = a_{T_2} - a_{I_2}$$

Then, the two-dimensional guidance law for the interceptor can be obtained similarly as

$$a_{I_1}^* = \frac{3T_{\text{go}}}{(1-\gamma^{-1})T_{\text{go}}^3 + 3c}(x_1 + T_{\text{go}} v_1) \tag{17a}$$

$$a_{I_2}^* = \frac{3T_{\text{go}}}{(1-\gamma^{-1})T_{\text{go}}^3 + 3c}(x_2 + T_{\text{go}} v_2) \tag{17b}$$

Note that the interceptor acceleration is independent in each direction. From Fig. 1, the LOS rate is

$$\dot{\lambda} = \frac{\mathrm{d}}{\mathrm{d}t}\left(\tan^{-1}\frac{x_2}{x_1} - \lambda_0\right) = \frac{x_1 v_2 - x_2 v_1}{x_1^2 + x_2^2} \tag{18}$$

where λ_0 is the angle between the nominal LOS and the x_1 axis. The closing velocity and time-to-go are

$$V_c \triangleq -\dot{R} = -\frac{\mathrm{d}}{\mathrm{d}t}\sqrt{x_1^2 + x_2^2} = -\frac{x_1 v_1 + x_2 v_2}{\sqrt{x_1^2 + x_2^2}} \tag{19a}$$

$$T_{\text{go}} \triangleq -\frac{R}{\dot{R}} = -\frac{x_1^2 + x_2^2}{x_1 v_1 + x_2 v_2} \tag{19b}$$

where R is the range and $\dot{R}$ is the range rate. Then, by using Eqs. (16), (18), and (19), Eq. (17) can be written as

$$\begin{bmatrix} a_{I_1}^* \\ a_{I_2}^* \end{bmatrix} = N V_c \dot{\lambda} \begin{bmatrix} \cos\left(\lambda + \lambda_0 + \frac{\pi}{2}\right) \\ \sin\left(\lambda + \lambda_0 + \frac{\pi}{2}\right) \end{bmatrix}$$

Note that this two-dimensional interceptor acceleration vector is orthogonal to the instantaneous LOS. Therefore, depending on the relative dynamics considered in the problem formulation, the interceptor acceleration can be applied in the direction that is orthogonal to either the nominal LOS or the instantaneous LOS.

III. Problem Formulation

Consider the one-dimensional relative dynamics in Eq. (7), but now the interceptor has a lag due to its autopilot. This lag is modeled by first-order dynamics with the pole at $-\alpha$ and the zero at $-\frac{\alpha}{\beta}$. That is, the transfer function of the lag is

$$\frac{a_I(s)}{\bar{a}_I(s)} = \frac{\beta s + \alpha}{s + \alpha} \tag{20}$$

where $\bar{a}_I$ is the interceptor acceleration command. It is sometimes important to include the zero in the lag. For example, tail-controlled missiles have a nonminimal phase zero that can be modeled with $\beta < 0$ [11]. Note that a lag without any zero is a special case of Eq. (20) with $\beta = 0$. The interceptor acceleration in Eq. (20) can be expressed as

$$a_I = (1-\beta)\tilde{a}_I + \beta \bar{a}_I \tag{21}$$

where

$$\dot{\tilde{a}}_I = -\alpha\tilde{a}_I + \alpha\bar{a}_I$$

If the interceptor's lag is included directly in the system dynamics, as suggested by [4,9,10], the linear-quadratic pursuit-evasion game becomes

$$\min_{\bar{a}_I}\max_{a_T}\left\{\frac{1}{2c}\bar{x}(t_f)^2 + \frac{1}{2}\int_{t_0}^{t_f}[\bar{a}_I(t)^2 - \gamma a_T(t)^2]\,\mathrm{d}t\right\} \tag{22}$$

subject to

$$\dot{\bar{x}} = v \tag{23a}$$

$$\dot{v} = a_T - (1-\beta)\tilde{a}_I - \beta\bar{a}_I \tag{23b}$$

$$\dot{\tilde{a}}_I = -\alpha\tilde{a}_I + \alpha\bar{a}_I \tag{23c}$$

In this problem formulation, because the system dynamics in Eq. (23) are known to both players, the target strategy is determined with knowledge about the interceptor's lag. Then, the target may maneuver at a small time-to-go to produce a large terminal miss, knowing that the interceptor will not have enough time to respond due to its lag. Therefore, if the weighting on the terminal miss (i.e., c^{-1}) is too large, the optimal cost could go to infinity, which means that the target will win the game even though the target is less maneuverable than the interceptor. This is consistent with the finite escape time of the associated Riccati equation [4,9,10]. To ensure the existence of an interceptor strategy, c^{-1} has to be chosen small enough so that the optimal cost will remain finite. However, this manipulation prevents the target from maximizing the terminal miss and effectively constrains the target strategy. Therefore, the interceptor strategy is derived against the worst-case target strategy that is not really the worst case. This interceptor strategy will not perform well against targets that intend to maximize the terminal miss. In Sec. VI.B, the numerical example shows that this interceptor strategy performs much worse than the classic interceptor strategy in Eq. (10), which does not consider the interceptor's lag, and the proportional navigation that considers the interceptor's lag.

IV. Optimal Interceptor Strategy Against Closed-Loop Target Strategy

To overcome this difficulty, a new approach is proposed, where the target strategy and interceptor strategy are determined separately in two optimization problems instead of together in one optimization problem. First, the target strategy is derived in the two-sided optimization problem that does not consider the interceptor's lag. This optimization problem is equivalent to the classic linear-quadratic pursuit-evasion game in Sec. II.B. By using Eqs. (5b) and (9), this target strategy is

$$a_T^* = \frac{1}{\gamma}\begin{bmatrix}0\\1\end{bmatrix}^T\left\{\frac{3}{(1-\gamma^{-1})T_{\mathrm{go}}^3 + 3c}\begin{bmatrix}1 & T_{\mathrm{go}}\\ T_{\mathrm{go}} & T_{\mathrm{go}}^2\end{bmatrix}\right\}\begin{bmatrix}\bar{x}\\ v\end{bmatrix} = \frac{1}{\gamma}B_2^T S x \tag{24}$$

where

$$x = \begin{bmatrix}\bar{x}\\ v\\ \tilde{a}_I\end{bmatrix}; \qquad B_2 = \begin{bmatrix}0\\1\\0\end{bmatrix}$$

$$S = \frac{3}{(1-\gamma^{-1})T_{\mathrm{go}}^3 + 3c}\begin{bmatrix}1 & T_{\mathrm{go}} & 0\\ T_{\mathrm{go}} & T_{\mathrm{go}}^2 & 0\\ 0 & 0 & 0\end{bmatrix}$$

By substituting Eq. (24) into Eq. (23),

$$\dot{x} = \left(A + \frac{1}{\gamma}B_2B_2^T S\right)x + B_1\bar{a}_I \tag{25}$$

where

$$A = \begin{bmatrix}0 & 1 & 0\\ 0 & 0 & -(1-\beta)\\ 0 & 0 & -\alpha\end{bmatrix}; \qquad B_1 = \begin{bmatrix}0\\-\beta\\ \alpha\end{bmatrix}$$

By substituting Eq. (24) into Eq. (22), the one-sided optimization problem for deriving the interceptor strategy in the presence of interceptor's lag is

$$\min_{\bar{a}_I}\left[\frac{1}{2}x(t_f)^T Q_f x(t_f) + \frac{1}{2}\int_{t_0}^{t_f}(x^T Q x + \bar{a}_I^2)\,\mathrm{d}t\right] \tag{26}$$

subject to Eq. (25), where

$$Q = -\frac{1}{\gamma}SB_2B_2^T S; \qquad Q_f = \begin{bmatrix}c^{-1} & 0 & 0\\ 0 & 0 & 0\\ 0 & 0 & 0\end{bmatrix}$$

By using the calculus of variations, the optimal solution is

$$\bar{a}_I^* = -B_1^T\bar{S}x \tag{27}$$

where $\bar{S}$ satisfies the Riccati equation:

$$-\dot{\bar{S}} = \bar{S}(A + \tfrac{1}{\gamma}B_2B_2^T S) + (A + \tfrac{1}{\gamma}B_2B_2^T S)^T\bar{S} - \tfrac{1}{\gamma}SB_2B_2^T S - \bar{S}B_1B_1^T\bar{S}$$

and $\bar{S}(t_f) = Q_f$.

In this new problem formulation, the target strategy in Eq. (24) is determined, assuming that the interceptor does not have a lag. Therefore, the interceptor strategy in Eq. (27), derived in the presence of interceptor's lag against this target strategy, is more realistic and effective. This is shown by the numerical example in Sec. VI.B. However, this problem formulation does not have a saddle point condition because of the additional dynamics of the interceptor's lag. Therefore, the interceptor strategy in Eq. (27) is considered as the worst-case design, where the target is perverse enough to determine its worst strategy but is not perverse enough to actually change its strategy as the game evolves [2]. In other words, it is implicitly assumed that the target plays first by announcing its strategy ahead of time. Note that, when $\alpha \to \infty$, the interceptor strategy in Eq. (27) is equivalent to the classic interceptor strategy in Eq. (10).

From Eq. (27), the guidance law for the interceptor can be written as

$$\bar{a}_I^* = (\beta\bar{S}_{12} - \alpha\bar{S}_{13})\bar{x} + (\beta\bar{S}_{22} - \alpha\bar{S}_{23})v + (\beta\bar{S}_{23} - \alpha\bar{S}_{33})\tilde{a}_I \tag{28}$$

where

$$\bar{S} = \begin{bmatrix}\bar{S}_{11} & \bar{S}_{12} & \bar{S}_{13}\\ \bar{S}_{12} & \bar{S}_{22} & \bar{S}_{23}\\ \bar{S}_{13} & \bar{S}_{23} & \bar{S}_{33}\end{bmatrix}$$

By using Eq. (14), Eq. (28) can be written as

$$\bar{a}_I^* = NV_c\dot{\lambda} + (\beta\bar{S}_{23} - \alpha\bar{S}_{33})\tilde{a}_I \tag{29}$$

where

$$N = T_{\mathrm{go}}^2(\beta\bar{S}_{12} - \alpha\bar{S}_{13}) = T_{\mathrm{go}}(\beta\bar{S}_{22} - \alpha\bar{S}_{23})$$

Note that this interceptor acceleration command is applied in the direction that is orthogonal to the nominal LOS. It can be shown similarly, as in remark 2, that if the two-dimensional relative dynamics are considered, the interceptor acceleration command will be applied in the direction that is orthogonal to the instantaneous LOS.

Remark 3: Another approach for deriving an effective interceptor strategy in the presence of the interceptor's lag is to further include the target's lag [4]. Then, the target cannot maneuver instantaneously at a small time-to-go to produce large terminal miss. However, because the target's lag is now included in the system dynamics, the implementation of the guidance law for the interceptor requires the estimation of the target acceleration. Furthermore, the interceptor

usually does not have knowledge about the target's lag in realistic situations.

V. Optimal Interceptor Strategy Against Open-Loop Target Strategy

Here, another interceptor strategy is derived similarly, but its second optimization problem considers the target strategy as an open-loop strategy instead of a closed-loop strategy. That is, the target strategy is a function of the state of the first optimization problem instead of in feedback form as a function of the state of the second optimization problem. From Eqs. (12b) and (13), the open-loop target strategy is

$$a_T^*(t) = \frac{T_{\text{go}}}{\gamma c}\bar{x}_1(t_f) \tag{30}$$

where

$$\bar{x}_1(t_f) = \left[1 + \frac{(1-\gamma^{-1})T_{\text{go}}^3}{3c}\right]^{-1}[\bar{x}_1(t) + T_{\text{go}}v_1(t)] \tag{31}$$

and the subscript 1 represents the state of the first optimization problem.

By substituting Eq. (30) into Eqs. (22) and (23), the one-sided optimization problem for deriving the interceptor strategy in the presence of the interceptor's lag is

$$\min_{\bar{a}_I}\left[\frac{1}{2c}\bar{x}_2(t_f)^2 + \frac{1}{2}\int_{t_0}^{t_f}\bar{a}_I(t)^2\,\mathrm{d}t\right]$$

subject to

$$\dot{\bar{x}}_2 = v_2 \tag{32a}$$

$$\dot{v}_2 = \frac{T_{\text{go}}}{\gamma c}\bar{x}_1(t_f) - (1-\beta)\tilde{a}_I - \beta\bar{a}_I \tag{32b}$$

$$\dot{\tilde{a}}_I = -\alpha\tilde{a}_I + \alpha\bar{a}_I \tag{32c}$$

where the subscript 2 represents the state of the second optimization problem. In this problem formulation, the target assumes that the interceptor plays optimally, as in the first optimization problem, and will not take advantage of any nonoptimal play made by the interceptor [2]. Therefore, the interceptor strategy derived against the open-loop target strategy satisfies a less stringent type of optimality than the interceptor strategy [Eq. (27)] derived against the closed-loop target strategy. However, this interceptor strategy can be solved in closed form as follows, which significantly reduces the computation.

To solve this optimization problem, the Hamiltonian is written as

$$\mathcal{H} = \frac{1}{2}\bar{a}_I^2 + \lambda_1 v_2 + \lambda_2\left[\frac{T_{\text{go}}}{\gamma c}\bar{x}_1(t_f) - (1-\beta)\tilde{a}_I - \beta\bar{a}_I\right] + \lambda_3(-\alpha\tilde{a}_I + \alpha\bar{a}_I)$$

where λ_1, λ_2, and λ_3 are Lagrange multipliers. From the first-order necessary condition, the optimal solution for the interceptor acceleration command is

$$\bar{a}_I^* = -\alpha\lambda_3 + \beta\lambda_2 \tag{33}$$

and the dynamic equations for the Lagrange multipliers are

$$\dot{\lambda}_1 = 0 \tag{34a}$$

$$\dot{\lambda}_2 = -\lambda_1 \tag{34b}$$

$$\dot{\lambda}_3 = \alpha\lambda_3 + (1-\beta)\lambda_2 \tag{34c}$$

where $\lambda_1(t_f) = \frac{1}{c}\bar{x}_2(t_f)$, $\lambda_2(t_f) = 0$, and $\lambda_3(t_f) = 0$. By integrating Eq. (34),

$$\lambda_1(t) = \frac{1}{c}\bar{x}_2(t_f) \tag{35a}$$

$$\lambda_2(t) = \frac{T_{\text{go}}}{c}\bar{x}_2(t_f) \tag{35b}$$

$$\lambda_3(t) = \frac{1-\beta}{\alpha^2 c}(1 - \alpha T_{\text{go}} - e^{-\alpha T_{\text{go}}})\bar{x}_2(t_f) \tag{35c}$$

By substituting Eq. (35) into Eq. (33), the interceptor strategy is

$$\bar{a}_I^*(t) = -\frac{1}{\alpha c}[1 - \beta - \alpha T_{\text{go}} - (1-\beta)e^{-\alpha T_{\text{go}}}]\bar{x}_2(t_f) \tag{36}$$

To implement Eq. (36), the interceptor acceleration command needs to be expressed in terms of the current state instead of the final state. By integrating Eq. (32c) with Eq. (36),

$$\tilde{a}_I(t) = e^{\alpha T_{\text{go}}}\tilde{a}_I(t_f) + \frac{1}{c}\left(T_{\text{go}} + \frac{\beta}{\alpha} - \frac{1+\beta}{2\alpha}e^{\alpha T_{\text{go}}} + \frac{1-\beta}{2\alpha}e^{-\alpha T_{\text{go}}}\right)\bar{x}_2(t_f) \tag{37}$$

By integrating Eq. (32b) with Eqs. (36) and (37),

$$v_2(t) = \frac{1-\beta}{\alpha}(e^{\alpha T_{\text{go}}} - 1)\tilde{a}_I(t_f) + v_2(t_f) + \frac{1}{2c}\left[T_{\text{go}}^2 + \frac{1-\beta^2}{\alpha^2}(2 - e^{\alpha T_{\text{go}}} - e^{-\alpha T_{\text{go}}})\right]\bar{x}_2(t_f) - \frac{T_{\text{go}}^2}{2\gamma c}\bar{x}_1(t_f) \tag{38}$$

By integrating Eq. (32a) with Eq. (38),

$$\bar{x}_2(t) = \frac{1-\beta}{\alpha^2}(1 + \alpha T_{\text{go}} - e^{\alpha T_{\text{go}}})\tilde{a}_I(t_f) - T_{\text{go}}v_2(t_f) + \frac{1}{2c}\left[2c - \frac{T_{\text{go}}^3}{3} - \frac{2(1-\beta^2)T_{\text{go}}}{\alpha^2} + \frac{1-\beta^2}{\alpha^3}(e^{\alpha T_{\text{go}}} - e^{-\alpha T_{\text{go}}})\right]\bar{x}_2(t_f) + \frac{T_{\text{go}}^3}{6\gamma c}\bar{x}_1(t_f) \tag{39}$$

Now, the current state is expressed in terms of the final state, as in Eqs. (37–39). By inverting these equations and using Eq. (31), $\bar{x}_2(t_f)$ can be expressed in terms of the current state as

$$\bar{x}_2(t_f) = \bar{c}\left[\bar{x}_2(t) + T_{\text{go}}v_2(t) + \frac{1-\beta}{\alpha^2}(1 - \alpha T_{\text{go}} - e^{-\alpha T_{\text{go}}})\tilde{a}_I(t) + \frac{T_{\text{go}}^3}{(\gamma-1)T_{\text{go}}^3 + 3\gamma c}\bar{x}_1(t) + \frac{T_{\text{go}}^4}{(\gamma-1)T_{\text{go}}^3 + 3\gamma c}v_1(t)\right] \tag{40}$$

where

$$\bar{c} = 2c\left[2c + \frac{1 + 2\beta - 3\beta^2}{\alpha^3} + \frac{2(1-\beta)^2T_{\text{go}}}{\alpha^2} - \frac{2(1-\beta)T_{\text{go}}^2}{\alpha} + \frac{2T_{\text{go}}^3}{3} - \frac{4(1-\beta)}{\alpha^2}\left(T_{\text{go}} + \frac{\beta}{\alpha}\right)e^{-\alpha T_{\text{go}}} - \frac{(1-\beta)^2}{\alpha^3}e^{-2\alpha T_{\text{go}}}\right]^{-1}$$

Then, by substituting Eq. (40) into Eq. (36) and letting $\bar{x} = \bar{x}_1 = \bar{x}_2$ and $v = v_1 = v_2$, the guidance law for the interceptor is obtained in closed form as

$$\bar{a}_I^*(t) = c^*\left[\frac{T_{\text{go}}^3 + 3c}{(1-\gamma^{-1})T_{\text{go}}^3 + 3c}\bar{x}(t) + \frac{T_{\text{go}}(T_{\text{go}}^3 + 3c)}{(1-\gamma^{-1})T_{\text{go}}^3 + 3c}v(t) + \frac{1-\beta}{\alpha^2}(1 - \alpha T_{\text{go}} - e^{-\alpha T_{\text{go}}})\tilde{a}_I(t)\right] \tag{41}$$

where

$$c^* = -\frac{2}{\alpha}[1-\beta-\alpha T_{\text{go}}-(1-\beta)e^{-\alpha T_{\text{go}}}]\left[2c+\frac{1+2\beta-3\beta^2}{\alpha^3}+\frac{2(1-\beta)^2 T_{\text{go}}}{\alpha^2}-\frac{2(1-\beta)T_{\text{go}}^2}{\alpha}+\frac{2T_{\text{go}}^3}{3}-\frac{4(1-\beta)}{\alpha^2}\left(T_{\text{go}}+\frac{\beta}{\alpha}\right)e^{-\alpha T_{\text{go}}}-\frac{(1-\beta)^2}{\alpha^3}e^{-2\alpha T_{\text{go}}}\right]^{-1}$$

Note that, when $\alpha \to \infty$, the interceptor strategy in Eq. (41) is equivalent to the classic interceptor strategy in Eq. (10). That is, in the limit when the time constant of the interceptor's lag goes to zero, this new guidance law is equivalent to the classic game-theoretic guidance law, which does not consider any lag.

By using Eq. (14), Eq. (41) can be written as

$$\bar{a}_I^* = NV_c\dot{\lambda} + \frac{c^*(1-\beta)}{\alpha^2}(1-\alpha T_{\text{go}}-e^{-\alpha T_{\text{go}}})\tilde{a}_I \tag{42}$$

where

$$N = \frac{c^* T_{\text{go}}^2(T_{\text{go}}^3+3c)}{(1-\gamma^{-1})T_{\text{go}}^3+3c} \tag{43}$$

and

$$\lim_{T_{\text{go}}\to\infty} N = \frac{3}{1-\gamma^{-1}}$$

Note that this interceptor acceleration command is applied in the direction that is orthogonal to the nominal LOS. It can be shown similarly, as in remark 2, that if the two-dimensional relative dynamics are considered, the interceptor acceleration command will be applied in the direction that is orthogonal to the instantaneous LOS.

Remark 4: For the purpose of comparison, the guidance law for the interceptor obtained by solving the optimization problem in Eq. (22) is

$$\bar{a}_I^*(t) = c^*\left[\bar{x}(t)+T_{\text{go}}v(t)+\frac{1-\beta}{\alpha^2}(1-\alpha T_{\text{go}}-e^{-\alpha T_{\text{go}}})\tilde{a}_I(t)\right] \tag{44}$$

where

$$c^* = -\frac{2}{\alpha}[1-\beta-\alpha T_{\text{go}}-(1-\beta)e^{-\alpha T_{\text{go}}}]\left[2c+\frac{1+2\beta-3\beta^2}{\alpha^3}+\frac{2(1-\beta)^2 T_{\text{go}}}{\alpha^2}-\frac{2(1-\beta)T_{\text{go}}^2}{\alpha}+\frac{2(1-\gamma^{-1})T_{\text{go}}^3}{3}-\frac{4(1-\beta)}{\alpha^2}\left(T_{\text{go}}+\frac{\beta}{\alpha}\right)e^{-\alpha T_{\text{go}}}-\frac{(1-\beta)^2}{\alpha^3}e^{-2\alpha T_{\text{go}}}\right]^{-1}$$

When $\beta = 0$, Eq. (44) is equivalent to the guidance law in [4]. Note that, when $\alpha \to \infty$, Eq. (44) is equivalent to Eq. (10). By using Eq. (14), Eq. (44) can be written as

$$\bar{a}_I^* = NV_c\dot{\lambda} + \frac{c^*(1-\beta)}{\alpha^2}(1-\alpha T_{\text{go}}-e^{-\alpha T_{\text{go}}})\tilde{a}_I \tag{45}$$

where

$$N = c^* T_{\text{go}}^2$$

Note that, when $\gamma \to \infty$, Eqs. (41) and (42) are equivalent to Eqs. (44) and (45) and are the proportional navigation that considers the interceptor's lag [3,4].

VI. Numerical Example

The proposed guidance laws in Eqs. (29) and (42) are compared with the guidance law in Eq. (45), which is similar to the guidance law in [4] and the classic game-theoretic guidance law in Eq. (15), which does not consider the interceptor's lag. The performance of these four guidance laws are evaluated against a maneuvering target. The three-dimensional intercept geometry is shown in Fig. 2 and Table 1. The initial interceptor velocity vector is chosen, such that the magnitude is 1000 ft/s and the orientation places the interceptor and target (if nonmaneuvering) on the collision triangle. The interceptor acceleration command vector is updated at 100 Hz, and its magnitude is limited below 10 g. The interceptor's lag in Eq. (20) is chosen with $\alpha = 2$ and $\beta = -0.2$. That is, the time constant of the lag is 0.5 s, and it has a nonminimal phase zero. The target starts maneuvering without any lag by pulling up vertically at different instances of the engagement. Specifically, the target acceleration vector is in the vertical plane that contains the target velocity vector, and its orientation is orthogonal to the target velocity vector with a constant magnitude of 5 g. In Fig. 2, the target starts maneuvering after 1 s into the engagement, and the interceptor uses the guidance law in Eq. (42).

Table 1 Initial conditions of target and interceptor

	Target	Interceptor
Position, ft	(1500, 2000, 2500)	(0, 0, 0)
Velocity, ft/s	(0, −1000, 0)	(480, −360, 800)

A. Guidance Law Implementation

To implement the guidance laws, the three-dimensional relative motion between the target and the interceptor is decomposed into two two-dimensional planes: the vertical plane that contains $\mathbf{e}_r$ and $\mathbf{e}_\phi$, and the horizontal plane that contains $\mathbf{e}_r$ and $\mathbf{e}_\theta$, as shown in Fig. 3 [12]. The coordinate frame $(\mathbf{e}_r, \mathbf{e}_\theta, \mathbf{e}_\phi)$ is derived from the inertial coordinate frame (X_1, X_2, X_3), first with the rotation around the X_3 axis by θ (azimuth) and then with the rotation around the intermediate X_2 axis by $-\phi$ (elevation), so that $\mathbf{e}_r$ is along the instantaneous LOS, and

$$\mathbf{e}_r = \begin{bmatrix}\cos\phi\cos\theta\\ \cos\phi\sin\theta\\ \sin\phi\end{bmatrix}; \qquad \mathbf{e}_\theta = \begin{bmatrix}-\sin\theta\\ \cos\theta\\ 0\end{bmatrix}$$

$$\mathbf{e}_\phi = \begin{bmatrix}-\sin\phi\cos\theta\\ -\sin\phi\sin\theta\\ \cos\phi\end{bmatrix}$$

The LOS rate vector is

$$\dot{\mathbf{e}}_r = \mathbf{w}\times\mathbf{e}_r = (\dot{\theta}\sin\phi\mathbf{e}_r - \dot{\phi}\mathbf{e}_\theta + \dot{\theta}\cos\phi\mathbf{e}_\phi)\times\mathbf{e}_r = \dot{\theta}\cos\phi\mathbf{e}_\theta + \dot{\phi}\mathbf{e}_\phi$$

where $\mathbf{w}$ is the angular velocity of the coordinate frame $(\mathbf{e}_r, \mathbf{e}_\theta, \mathbf{e}_\phi)$ with respect to the coordinate frame (X_1, X_2, X_3). Then, the LOS rate in the vertical plane $(\mathbf{e}_r, \mathbf{e}_\phi)$ is $\dot{\phi}$, and the LOS rate in the horizon plane $(\mathbf{e}_r, \mathbf{e}_\theta)$ is $\dot{\theta}\cos\phi$. Therefore, the three-dimensional interceptor acceleration command vector is

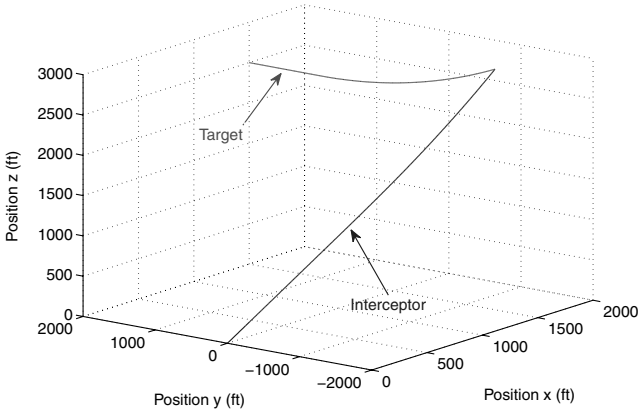

Fig. 2 Example trajectories of target and interceptor.

$$\bar{a}_{I_\phi}\mathbf{e}_\phi + \bar{a}_{I_\theta}\mathbf{e}_\theta \tag{46}$$

where $\bar{a}_{I_\phi}$ and $\bar{a}_{I_\theta}$ are obtained by using the guidance law in Eqs. (29), (42), and (45) or Eq. (15) with $\dot{\lambda} = \dot{\phi}$ and $\dot{\lambda} = \dot{\theta}\cos\phi$, respectively. Note that, when the design weightings for the two two-dimensional guidance laws are chosen to be the same, Eq. (46) is equivalent to the interceptor acceleration command in [12] when the interceptor's lag is not considered.

To generate the simulation results in Sec. VI.B, it is assumed that perfect information is available. That is, the relative position x_1, x_2, x_3, and the relative velocity v_1, v_2, and v_3 are known perfectly. In practice, they can be estimated by using the game-theoretic filters in [8,13], which are derived based on the linear-exponential-Gaussian differential game with different information patterns solved in [14,15]. Then, the LOS rates can be obtained by using

$$\dot{\phi} = \frac{\mathrm{d}}{\mathrm{d}t}\left(\sin^{-1}\frac{x_3}{\sqrt{x_1^2+x_2^2+x_3^2}}\right) = \frac{(x_1^2+x_2^2)v_3 - x_3(x_1v_1+x_2v_2)}{\sqrt{x_1^2+x_2^2}(x_1^2+x_2^2+x_3^2)} \tag{47a}$$

$$\dot{\theta} = \frac{\mathrm{d}}{\mathrm{d}t}\left(\tan^{-1}\frac{x_2}{x_1}\right) = \frac{x_1v_2 - x_2v_1}{x_1^2+x_2^2} \tag{47b}$$

The closing velocity and time-to-go can be obtained by using

$$V_c = -\dot{R} = -\frac{\mathrm{d}}{\mathrm{d}t}\sqrt{x_1^2+x_2^2+x_3^2} = -\frac{x_1v_1+x_2v_2+x_3v_3}{\sqrt{x_1^2+x_2^2+x_3^2}} \tag{48a}$$

$$T_{\mathrm{go}} = -\frac{R}{\dot{R}} = -\frac{x_1^2+x_2^2+x_3^2}{x_1v_1+x_2v_2+x_3v_3} \tag{48b}$$

It is also assumed that $\tilde{a}_{I_\phi}$ and $\tilde{a}_{I_\theta}$ are known perfectly. In practice, they can be obtained by using Eq. (21), where a_{I_ϕ} and a_{I_θ} are measured and $\bar{a}_{I_\phi}$ and $\bar{a}_{I_\theta}$ are known.

Remark 5: If the three-dimensional relative dynamics, as shown in Fig. 3, are considered instead of the decomposition into two two-dimensional relative dynamics, the three-dimensional guidance law for the interceptor can be obtained, similarly to Eq. (41), as

$$\bar{a}_{I_1}^* = c^*\left[\frac{T_{\mathrm{go}}^3+3c}{(1-\gamma^{-1})T_{\mathrm{go}}^3+3c}x_1 + \frac{T_{\mathrm{go}}(T_{\mathrm{go}}^3+3c)}{(1-\gamma^{-1})T_{\mathrm{go}}^3+3c}v_1 + \frac{1-\beta}{\alpha^2}(1-\alpha T_{\mathrm{go}} - e^{-\alpha T_{\mathrm{go}}})\tilde{a}_{I_1}\right] \tag{49a}$$

$$\bar{a}_{I_2}^* = c^*\left[\frac{T_{\mathrm{go}}^3+3c}{(1-\gamma^{-1})T_{\mathrm{go}}^3+3c}x_2 + \frac{T_{\mathrm{go}}(T_{\mathrm{go}}^3+3c)}{(1-\gamma^{-1})T_{\mathrm{go}}^3+3c}v_2 + \frac{1-\beta}{\alpha^2}(1-\alpha T_{\mathrm{go}} - e^{-\alpha T_{\mathrm{go}}})\tilde{a}_{I_2}\right] \tag{49b}$$

$$\bar{a}_{I_3}^* = c^*\left[\frac{T_{\mathrm{go}}^3+3c}{(1-\gamma^{-1})T_{\mathrm{go}}^3+3c}x_3 + \frac{T_{\mathrm{go}}(T_{\mathrm{go}}^3+3c)}{(1-\gamma^{-1})T_{\mathrm{go}}^3+3c}v_3 + \frac{1-\beta}{\alpha^2}(1-\alpha T_{\mathrm{go}} - e^{-\alpha T_{\mathrm{go}}})\tilde{a}_{I_3}\right] \tag{49c}$$

Note that the interceptor acceleration command is independent in each direction. By using Eqs. (43), (47), and (48), it can be shown that Eq. (49) is equivalent to Eq. (46) when the design weightings for the two two-dimensional guidance laws are chosen to be the same. Note that this is also shown in [16] in a more compact way by expressing the guidance law in the vector form when the interceptor's lag is not considered.

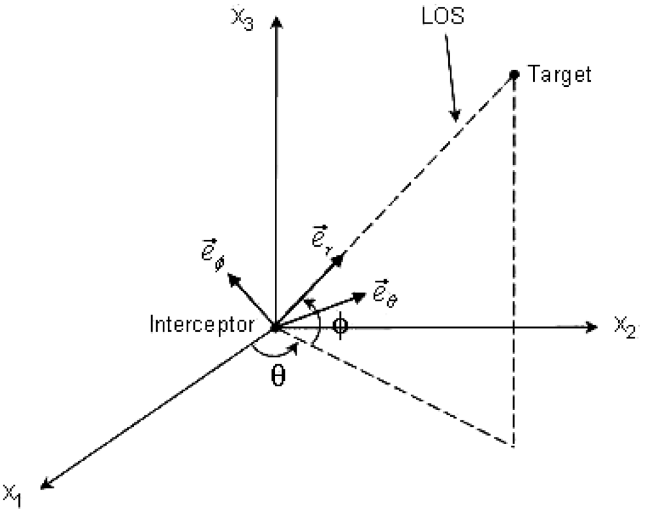

Fig. 3 Three-dimensional relative motion between target and interceptor.

B. Simulation Results

To determine the best performance and understand the behavior of the four guidance laws, a range of design weightings (i.e., γ and c) are applied. Because γ and c have a one-to-one relationship with the navigation ratio when $T_{\mathrm{go}} \to \infty$ (denoted as N_{ss}) and the maximal navigation ratio (denoted as $N_{\max}$), N_{ss} and $N_{\max}$ are used as the

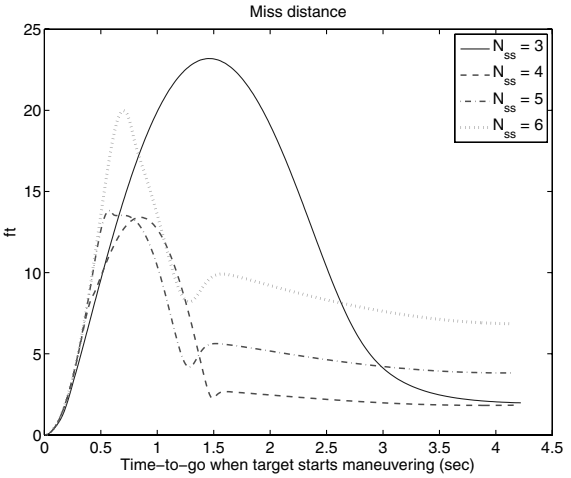

a) Target starts maneuvering at different time-to-go

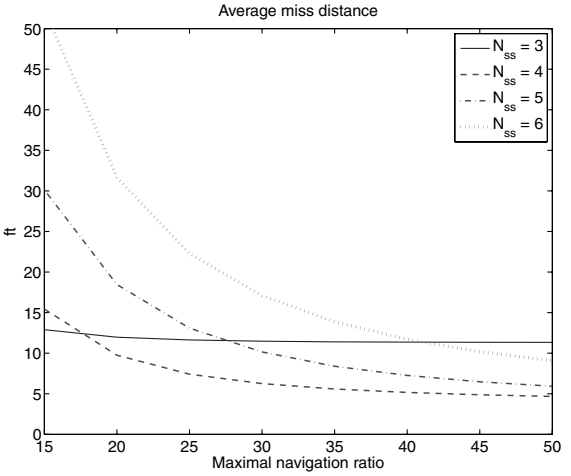

b) Different maximal navigation ratios

Fig. 4 Miss distance results for guidance law in Eq. (29).

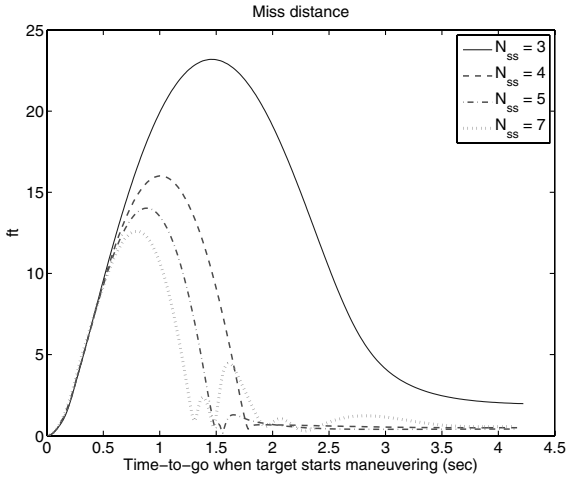

a) Target starts maneuvering at different time-to-go

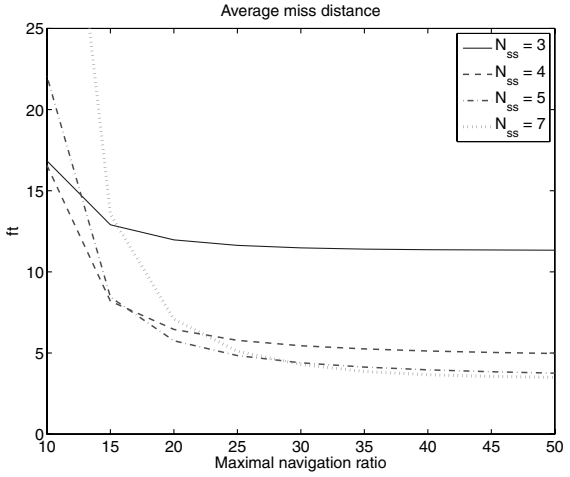

b) Different maximal navigation ratios

Fig. 5 Miss distance results for guidance law in Eq. (42).

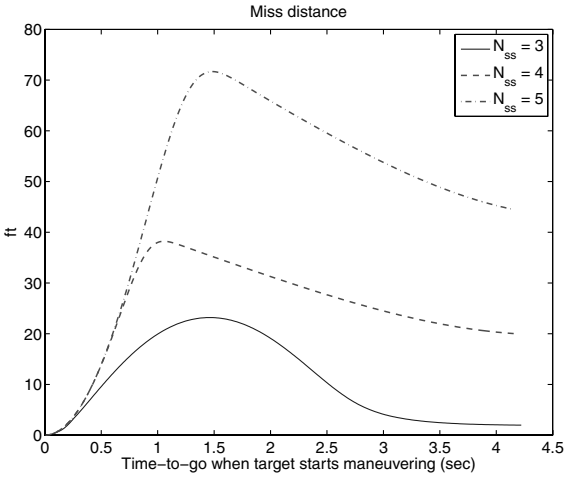

a) Target starts maneuvering at different time-to-go

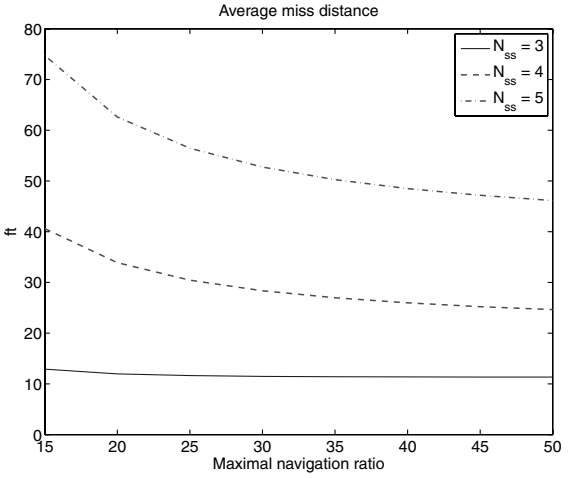

b) Different maximal navigation ratios

Fig. 6 Miss distance results for guidance law in Eq. (45).

independent variables instead of γ and c for the parametric study because of their physical meanings and importance. Furthermore, the maximal navigation ratio is limited below 50 to be practical, while results with a higher maximal navigation ratio can be inferred.

For the proposed guidance law in Eq. (29), with $N_{\max} = 50$, Fig. 4a shows the miss distance versus the time-to-go when the target starts maneuvering. It is shown that Eq. (29) has the best performance when $N_{ss} \approx 4$. Note that when $N_{ss} = 3$, $\gamma \to \infty$, and it is equivalent to the proportional navigation that considers the interceptor's lag. By averaging the miss distance over the entire range of the time-to-go when the target starts maneuvering, Fig. 4b shows the average miss distance versus the maximal navigation ratio. It is shown that Eq. (29) has the best performance when $N_{ss} \approx 4$ and $N_{\max} \geq 35$.

For the proposed guidance law in Eq. (42), with $N_{\max} = 50$, Fig. 5a shows the miss distance versus the time-to-go when the target starts maneuvering. It is shown that Eq. (42) has the best performance when $5 \leq N_{ss} \leq 7$. Note that when $N_{ss} = 3$, it is equivalent to the proportional navigation that considers the interceptor's lag. Figure 5b shows the average miss distance versus the maximal navigation ratio. It is shown that Eq. (42) has the best performance when $5 \leq N_{ss} \leq 7$ and $N_{\max} \geq 35$. From Figs. 4 and 5, the guidance law in Eq. (42) performs better than the guidance law in Eq. (29).

For the guidance law in Eq. (45), which is similar to the guidance law in [4], Fig. 6a shows the miss distance with $N_{\max} = 50$ versus the time-to-go when the target starts maneuvering, and Fig. 6b shows the average miss distance versus the maximal navigation ratio. It is shown that Eq. (45) has the best performance when $N_{ss} = 3$, where it is equivalent to the proportional navigation that considers the interceptor's lag. Therefore, Eq. (45) performs worse than the proportional navigation that considers the interceptor's lag. While only one target maneuver and one intercept geometry are considered here, the poor performance of Eq. (45) is uncharacteristic for a game-theoretic guidance law, which is designed conservatively by considering the worst-case target strategy. As discussed earlier, this is because Eq. (45) exists only when c^{-1} is small and is derived against the worst-case target strategy that is not really the worst case. Although this approach is mathematically correct, its interpretation of the differential game and application to the missile intercept problem are clearly inappropriate. From Figs. 4–6, the guidance laws in Eqs. (29) and (42) perform significantly better than the guidance law in Eq. (45) by correctly taking into account the interceptor's lag.

For the classic game-theoretic guidance law Eq. (15), which does not consider the interceptor's lag, $c \to 0$ is chosen and the navigation ratio becomes a constant for which the value depends on γ. Figure 7 shows the miss distance versus the time-to-go when the target starts maneuvering. It is shown that Eq. (15) has the best performance when $5 \leq N \leq 10$. Note that, when $N = 3$, it is equivalent to the proportional navigation that does not consider the interceptor's lag. From Figs. 6 and 7, the guidance law in Eq. (45) performs much worse than the guidance law in Eq. (15), even though Eq. (45) considers the interceptor's lag while Eq. (15) does not. Furthermore, from Figs. 4, 5, and 7, the guidance laws in Eqs. (29) and (42) perform significantly better than the guidance law in Eq. (15) by considering the interceptor's lag.

Finally, Fig. 8 shows the navigation ratio of the guidance laws in Eqs. (29), (42), and (45) versus the time-to-go where $N_{ss} = 4$, 5 and 4, respectively, and $N_{\max} = 50$. When the time-to-go is small, the navigation ratio of Eq. (45) is very small, which indicates an

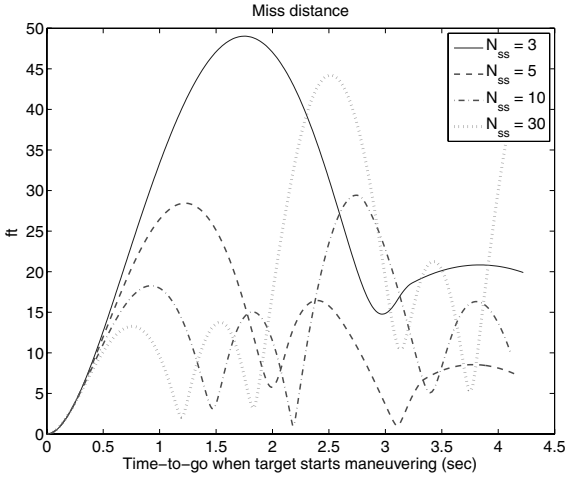

Fig. 7 Miss distance results for guidance law in Eq. (15).

ineffective guidance law, because the interceptor acceleration is not commanded in the last second before intercept. This explains the poor performance of Eq. (45), shown in Fig. 6, where the target is always maneuvering. Furthermore, the better performance of the guidance law in Eq. (42) over Eq. (29), shown in Figs. 4 and 5, is probably because the maximal navigation ratio of Eq. (42) occurs closer to the intercept than Eq. (29). Finally, to compensate the initial response of the interceptor acceleration in the opposite direction of the interceptor acceleration command due to the nonminimal phase zero, the navigation ratio is negative when the time-to-go is very small. Note that if the guidance laws do not consider the nonminimal phase zero, the navigation ratio will always be positive.

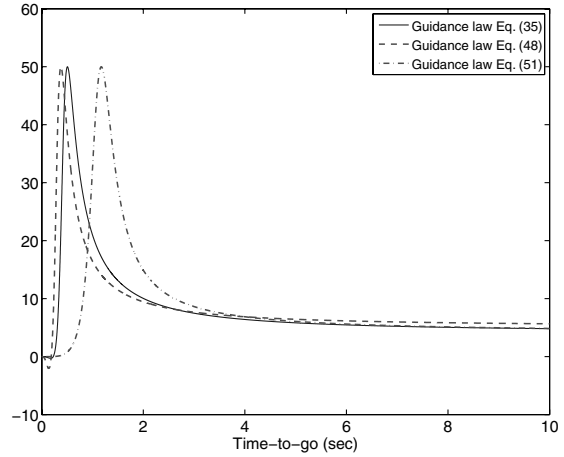

a) Normal view

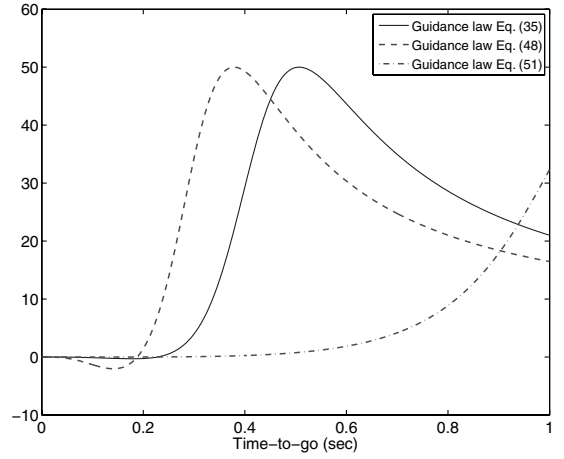

b) Zoomed view

Fig. 8 Navigation ratio of three guidance laws.

VII. Conclusions

It is revealed that the game-theoretic guidance law that considers the lag previously published in many papers and books performs poorly against targets that try to maximize the terminal miss. In particular, it performs worse than the classic game-theoretic guidance law, which does not consider the lag, and the proportional navigation that considers the lag. The problem is identified as the incorrect and unrealistic assumption that the target has knowledge about the interceptor's lag. Therefore, two new guidance laws are derived against targets that do not have knowledge about the interceptor's lag. Although there exists no saddle point condition for these two guidance laws, they can be considered as the worst-case design, where the target plays first by announcing its strategy ahead of time. The numerical example shows that these two new guidance laws improve the game-theoretic guidance law for homing missiles by correctly taking into account the autopilot lag.

References

[1] Yuan, L. C.-L., "Homing and Navigational Courses of Automatic Target-Seeking Devices," *Journal of Applied Physics*, Vol. 19, No. 12, Dec. 1948, pp. 1122–1128. doi:10.1063/1.1715028

[2] Bryson, A. E., Jr., and Ho, Y.-C., *Applied Optimal Control: Optimization, Estimation, and Control*, Hemisphere, New York, 1975, pp. 154–155, 277–288.

[3] Zarchan, P., *Tactical and Strategic Missile Guidance*, AIAA, Reston, VA, 2002, pp. 143–161.

[4] Ben-Asher, J. Z., and Yaesh, I., *Advances in Missile Guidance Theory*, AIAA, Reston, VA, 1998, pp. 1–5, 25–43, 89–102.

[5] Cottrell, R. G., "Optimal Intercept Guidance for Short-Range Tactical Missiles," *AIAA Journal*, Vol. 9, No. 7, July 1971, pp. 1414–1415. doi:10.2514/3.6369

[6] Garber, V., "Optimum Intercept Laws for Accelerating Targets," *AIAA Journal*, Vol. 6, No. 11, Nov. 1968, pp. 2196–2198. doi:10.2514/3.4962

[7] Speyer, J. L., Kim, K. D., and Tahk, M., "Passive Homing Missile Guidance Law Based on New Target Maneuver Models," *Journal of Guidance, Control, and Dynamics*, Vol. 13, No. 5, Sep.–Oct. 1990, pp. 803–812. doi:10.2514/3.25405

[8] Chen, R. H., Speyer, J. L., and Lianos, D., "Homing Missile Guidance and Estimation Under Agile Target Acceleration," *Journal of Guidance, Control, and Dynamics*, Vol. 30, No. 6, Nov.–Dec. 2007, pp. 1577–1589. doi:10.2514/1.30107

[9] Gutman, S., "On Optimal Guidance for Homing Missiles," *Journal of Guidance, Control, and Dynamics*, Vol. 2, No. 4, July–Aug. 1979, pp. 296–300. doi:10.2514/3.55878

[10] Gutman, S., *Applied Min–Max Approach to Missile Guidance and Control*, AIAA, Reston, VA, 2005.

[11] Palumbo, N. F., Reardon, B. E., and Blauwkamp, R. A., "Integrated Guidance and Control for Homing Missiles," *Johns Hopkins APL Technical Digest*, Vol. 25, No. 2, 2004, pp. 121–139.

[12] Yang, C.-D., and Yang, C.-C., "Analytical Solution of Three-Dimensional Realistic True Proportional Navigation," *Journal of Guidance, Control, and Dynamics*, Vol. 19, No. 3, May–June 1996, pp. 569–577. doi:10.2514/3.21659

[13] Chen, R. H., Speyer, J. L., and Lianos, D., "Terminal and Boost Phase Intercept of Ballistic Missile Defense," AIAA Guidance, Navigation and Control Conference, AIAA Paper 2008-6492, 2008.

[14] Swarup, A., and Speyer, J. L., "Linear-Quadratic-Gaussian Differential Games with Different Information Patterns," *Proceedings of the 42nd IEEE Conference on Decision and Control*, IEEE Publ., Piscataway, NJ, 2003, pp. 4146–4151.

[15] Swarup, A., and Speyer, J. L., "Characterization of LQG Differential Games with Different Information Patterns," *Proceedings of the 43nd IEEE Conference on Decision and Control*, IEEE Publ., Piscataway, NJ, 2004, pp. 3459–3466.

[16] Lam, V. C., "Acceleration-Compensated Zero-Effort-Miss Guidance Law," *Journal of Guidance, Control, and Dynamics*, Vol. 30, No. 4, July–Aug. 2007, pp. 1159–1162. doi:10.2514/1.26948